Available online at www.sciencedirect.com
ScienceDirect
International Journal of Pharmaceutics 348 (2008) 115–124
INTERNATIONAL JOURNAL OF PHARMACEUTICS
www.elsevier.com/locate/ijpharm

Pharmaceutical Nanotechnology

Incorporation of novel 1-alkylcarbonyloxymethyl prodrugs of 5-fluorouracil into poly(lactide-*co*-glycolide) nanoparticles

P.A. McCarron *, M. Hall

School of Pharmacy, Queen's University Belfast, Medical Biology Centre, 97 Lisburn Road, Belfast BT9 7BL, UK

Received 2 March 2007; received in revised form 2 July 2007; accepted 3 July 2007
Available online 18 July 2007

Abstract

Incorporation of 1-alkylcarbonyloxymethyl prodrugs of 5FU into poly(lactide-*co*-glycolide) nanoparticles using nanoprecipitation methods gave increased loading efficiencies over that obtained using the parent drug substance. SEM studies revealed spherical nanoparticles of around 200 nm in diameter, corresponding well with measurements made using photon correlation spectroscopy. The C_7 prodrug gave the best mean loading of 47.23%, which compared favourably to 3.68% loading achieved with 5FU. Loading efficiency was seen to follow the hydrophilic–lipophilic balance in the homologue series, where increases in lipophilicities alone were not good predictors of loading. Drug release, in terms of resultant 5FU concentration, was monitored using a flow-through dissolution apparatus. Cumulative drug release from nanoparticles loaded with the C_5 prodrug was linear over 6 h, with approximately 14% of the total available 5FU dose released and with no evidence of a burst effect. The flux profile of the C_5-loaded nanoparticles showed an initial peak in flux in the first sampling interval, but became linear for the remainder of the release phase. C_7-loaded nanoparticles released considerably less (4% in 6 h) with a similar flux pattern to that seen with the C_5 prodrug. The C_9-loaded nanoparticles released less than 1% of the available 5FU over 6 h, with a similar zero-order profile. The C_7 prodrug was deemed to be the prodrug of choice, achieving the highest loadings and releasing 5FU, following hydrolysis, in a zero-order fashion over a period of at least 6 h. Given the lack of burst effect and steady-state flux conditions, this nanoparticulate formulation offers a better dosing strategy for sustained intravenous use when compared to that arising from nanoparticles made by direct incorporation of 5FU.

Keywords: Nanoparticle; Fluorouracil; Prodrug; Alkylcarbonyloxymethyl; Poly(lactide-*co*-glycolide)

1. Introduction

Fluorouracil (5-fluoropyridrimidine-2,4(1*H*,3*H*)-dione; 5FU) is an analogue of the naturally occurring pyrimidine, uracil, with fluorine substitution in the 5 position, as illustrated in Fig. 1(a). It has accrued a long clinical history as both a palliative and therapeutic treatment modality for a variety of carcinomas, especially those involving the breast, colorectal region and skin (Grem, 2000). The drug acts by interfering with thymidylate synthesis and, consequently, with the synthesis of DNA (Rang et al., 1995), resulting in conversion to the fraudulent nucleotide, fluorodeoxyuridine monophosphate. Fluoridation of the C5 position, where methylation would normally occur, precludes conversion into thymidylate by thymidylate synthetase. The result is selective inhibition of DNA synthesis, with no effect on RNA or protein production (Rang et al., 1995). Administration of the drug is usually by intravenous bolus or continuous infusion as 5FU demonstrates unpredictable bioavailability, possibly related to variable first-pass metabolism, upon oral administration (Yuasa et al., 1996). Toxicity with 5FU is unusual, but may include myelosupression, mucositis and, rarely, a cerebellar syndrome (Schmoll et al., 1999).

Many differing techniques have been used to incorporate anti-cancer agents into nanoparticles (NP), with both pre-formed polymers and monomers being used in their manufacture (Brigger et al., 2002). Besides difficulties in the administration of such NP to specific sites of the body due to opsonisation, problems still remain in the formulation of some nanoparticulate systems with an adequately high and effective drug loading. This is especially the case with water-soluble drugs, such as 5FU. McCarron et al. (2000) found that most 5FU loaded into poly(*n*-butylcyanoacrylate) NP was actually surface-bound, with washing of NP in aqueous solvents removing most of the

* Corresponding author. Tel.: +44 2890 335800; fax: +44 2890 247794.
E-mail address: p.mccarron@qub.ac.uk (P.A. McCarron).

0378-5173/$ – see front matter © 2007 Elsevier B.V. All rights reserved.
doi:10.1016/j.ijpharm.2007.07.014

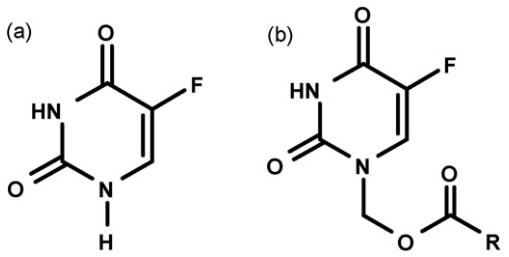

Fig. 1. Chemical structure of (a) 5FU and (b) the 1-ACOM prodrugs of 5FU, where R is an homologous series from CH_3 to C_9H_{19}.

adsorbed drug. It was postulated that the poor incorporation of 5FU was directly related to its hydrophilicity, as there was no dynamic for the drug to migrate into the nascent lipophilic polymer phase during NP creation. While it is possible to modify preparation conditions in a systematic fashion using response surface methodology to enhance the loading of a particular drug, there is a limit to what can be achieved with this type of optimisation process. Computer modelling has been used to determine the optimal condition for loading of 5FU with the emulsion polymerisation technique (McCarron et al., 1999). The loading of 5FU was optimised for this method by altering surfactant type, pH and monomer concentration, but still could be raised no higher than 0.68% (w/w). Although the drug has two pK_a values, which are relatively high at pH 8 and 13, being in the unionised state in acidic continuous phases is clearly not sufficient to promote incorporation.

If the parent drug substance has unsuitable physicochemical characteristics that are not conducive to high loadings, then incorporation of an apposite prodrug may be one strategy to overcome these difficulties. Prodrugs are transformed normally after administration to form a pharmacologically active species, by means of either metabolism or spontaneous chemical degradation (Denny, 2001). This a common strategy encountered in cancer chemotherapy, where research has focused on the production of prodrugs that are activated in neoplastic cells selectively (Chari, 1998; Dubois et al., 2002). Other areas of drug delivery, such as dermal and transdermal delivery, have also found the use of prodrugs to be beneficial. Their use in this area centres upon attenuating drug hydrophilicity, which beforehand would have been prohibitively high and militated against effective partitioning into the lipophilic dermal and epidermal environments (Chan and Li Wan Po, 1989). Indeed, a number of compounds have exhibited increased permeation by the addition of side-groups, including naproxen (Rautio et al., 2000), ketoprofen (Bonina et al., 2001), nalidixic acid (Bundgaard et al., 1989) and metronidazole (Johansen et al., 1986). Of interest in this research is the use of prodrugs of 5FU to alter the physiochemical characteristics of the drug. An assortment of prodrugs of 5FU have been synthesised, including 5′-deoxy-5-fluorouridine, capecitabine, BOF-A2, ftorafur, UFT and S-1 (Malet-Martino et al., 2002), mostly aimed at attenuating the side-effects experienced during chemotherapy.

The first report of the use of prodrugs of 5FU to enhance its topical delivery was by Mollgaard et al. (1982), where the percutaneous permeation characteristics of two *N*-1-acyloxymethyl derivatives of 5FU were determined and compared with that of 5FU *per se*. The prodrugs, especially the 1-butyryloxymethyl-5-fluorouracil derivative, showed improved permeation through the human skin compared with 5FU. Also, they were delivered in the form of parent drug due to cutaneous metabolism, mediated by hydrolytic enzymes. This work was furthered by Buur and Bundgaard (1984), who produced a series of prodrugs, including *N*-acyl, *N*-ethoxy- and *N*-phenoxycarbonyloxymethyl derivatives (Buur et al., 1986). A number of species were reported that had both increased water and lipid solubilities, which is of importance in the topical administration of the drug. However, it was Beall and Sloan who first produced a homologous series of these 1-alkylcarbonyl prodrugs in order to characterise their delivery fully (Beall et al., 1994; Beall and Sloan, 1996). These prodrugs proved very effective in the delivery of 5FU, but proved unstable in the presence of water or protic solvents. This led to the creation of the 1-alkylcarbonyloxymethyl (1-ACOM) prodrugs of 5FU, which possessed long half-lives, usually in excess of 100 h in the presence of water (Taylor and Sloan, 1998). The structure of 1-ACOM prodrugs of 5FU is shown in Fig. 1(b).

The main aim of this work was the incorporation of 1-alkylcarbonyloxymethyl prodrugs of 5FU into poly(lactide-*co*-glycolide) (PLGA) NP using the nanoprecipitation technique. By using prodrugs, where the lipophilicity of the parent compound is adjusted, it was hoped to achieve nanoparticulate drug loadings needed for effective drug delivery. After developing a suitable method for NP manufacture, a preliminary study using a homologous series of six 1-ACOM prodrugs ranging from C_1 to C_9 was performed, to assess suitability in terms of drug loading. Drug loading was examined in terms of 5FU content and release, necessitating prodrug hydrolysis using base to generate the parent compound. Base was also used in the pellet studies to degrade polymer and release prodrug. NP were characterised with respect to size, zeta potential and polydispersity and visualised using scanning electron microscopy. A novel in-line flow-through cell was used to evaluate drug release, which unlike the centrifugation-based methods of analysis, allowed a more rapid assessment of drug release with respect to time.

2. Materials and methods

2.1. Materials

Poly(D,L-lactide-*co*-glycolide) (PLGA; Resomer RG505) was a gift from Boehringer Ingelheim (Germany). Pluronic® F68 (Poloxamer 188) was a gift from BASF Corporation (New Jersey, USA). 1-ACOM prodrugs of 5FU were a gift from Dr. K Sloan, Department of Medicinal Chemistry, University of Florida, Gainsville, Florida. Full synthesis and characterisation have been described elsewhere (Taylor and Sloan, 1998). All solvents were of HPLC grade and reagents were of appropriate analytical quality. HPLC grade water was produced by filtration through a Milli-Q reagent water system (Millipore Ltd., Harrow, UK).

2.2. Preparation of drug-loaded NP

Drug-loaded NP were prepared using a nanoprecipitation procedure based upon that described by Govender et al. (1999). PLGA (100 mg) was dissolved in 10 ml of acetone. Prodrugs were weighed accurately using a micro-balance (Mettler MT5, Mettler-Toledo International Inc., Zürich) to approximately 4.0 mg, dissolved in the polymer solution and poured immediately into a stirred, aqueous solution of 0.5% (w/v) Poloxamer 188, previously filtered through a 0.22 μm poly(carbonate) filter (Millipore U.K. Ltd., Watford). The resulting cloudy suspension was transferred expeditiously to a round-bottomed flask and evaporated under reduced pressure for 20 min at 40 °C. The final volume was checked and made up to 10 ml with distilled water, if necessary.

2.3. Determination of drug loading and stability

Chromatographic analysis (HPLC) of 5FU was performed using a 4.6 mm × 250.0 mm Waters Spherisorb® 5 μm ODS2 analytical column. The mobile phase consisted of 25 mM acetate buffer (pH 5.0) in methanol (9:1) eluting at 1.0 ml min^{-1} (Schimadzu LC 10 AT VP). The injection volume used was 20 μl (Shimadzu SIL-10AD VP Auto Injector and CL-10A system controller) with ultraviolet detection at 266 nm (Shimadzu SPD-10A VP UV/Vis Detector). Calibration curves for 5FU in mobile phase were constructed in the concentration ranges 0–10 and 0–100 μg ml^{-1} to verify linearity of response.

Drug loading in NP was determined by analysing both the supernatant and particulate fractions obtained after ultracentrifugation (Sigma 3K30, Sigma laborzentrifugen GmbH, Osterode, Germany) of a given suspension. The 1-ACOM prodrugs used in this work are susceptible to hydrolysis in aqueous media, making their accurate determination difficult during protracted periods of centrifugation. Therefore, determination of loadings was based on 5FU analysis instead following accelerated hydrolysis of prodrug using sodium hydroxide. In order to determine the appropriate length of time required for complete prodrug hydrolysis, the lyophilised pellet fraction (2.0 mg) and supernatant (1.0 ml) containing the most stable prodrug (C_7) were subjected to 5.0 ml of 1.0 M and 1.0 ml of 2.0 M sodium hydroxide, respectively. These reactions were performed in a HPLC vial, which permitted regular autosampling (20 μL) over a period of several hours, allowing a determination of the time required to generate all 5FU from prodrugs to be established. As this method subjects 5FU to strongly basic conditions, a degradation study over the same time period was used to validate its stability over the duration of the analysis. A solution of 5FU of known concentration (50 μg ml^{-1}) was mixed with a 1.0 M solution of sodium hydroxide and monitored for 2 h using regular autosampling.

Loadings were determined by extraction from pelleted fractions and hydrolysis to 5FU. The pellet fraction was freeze dried (Edwards Modulyo, BOC Ltd., Crawley, UK) for 24 h and an accurately weighed sample (4.0 mg) re-suspended in 5.0 ml of 1 M sodium hydroxide. After 70 min, the solution was analysed using HPLC. The stabilities of prodrug-loaded NP, stored in lightproof sealable containers, were determined at two temperatures, namely 25 and 37 °C. Samples were analysed immediately after freeze drying and then at 28, 56 and 84 days later. Prodrug loading in the nanoparticulate fraction was expressed as a percentage of the theoretical maximum concentration of prodrug per milligram of NP, as shown in Eq. (1):

$$\%\ \text{prodrug loading} = \frac{\text{mass of prodrug (μg) per unit mass of freeze-dried NP}}{\text{total mass of prodrug (μg) used per unit mass of added polymer}} \quad (1)$$

Corresponding concentrations of non-entrapped prodrug in the supernatant were determined using a similar procedure to that above, so that when both determinations were summated, a check could be made that the two approximate to the total mass of prodrug added during the nanoparticulate formation procedure. A 5.0 ml sample of nanoparticulate suspension was centrifuged for 20 min at 57,000 × *g* and the supernatant removed. Supernatant (1.0 ml) was added to 1.0 ml of 2 M NaOH and left for 30 min. A sample of this solution was then analysed for 5FU using HPLC.

2.4. Sizing, zeta potential and polydispersity analysis

NP suspension (1.0 ml) was added to 50 ml of distilled and filtered water. After sonication – to both disperse and degas the suspension – photon correlation spectroscopy (Zetasizer 4 Malvern Instruments Ltd., Malvern, UK) was used to size the sample using light scattering from a laser source (633 nm) determined at a fixed angle (90°). Calibration of the instrument was carried out with a Duke Scientific certified polystyrene nanosphere® size standard (NIST traceable, 220 ± 6 nm). The zeta potential of the particle suspension was determined using laser anemometry after calibration of the instrument with a Malvern zeta potential standard (−50 ± 5 mV).

2.5. Scanning electron microscopy study

NP were visualised using scanning electron microscopy (Jeol JSM-6400) employing a 15 kV accelerating voltage, 10 mm working distance and resolution of 1024 × 1024. Freeze-dried nanoparticulate samples were dusted onto a double-sided adhesive pad applied to an aluminium stub. Excess sample was removed and the stub sputter coated with a 30 nm layer of gold. NP suspensions were visualised by adding the suspension directly to the aluminium stub and allowed to air-dry before sputter coating.

2.6. Drug release studies

An in-line flow-through diffusion cell arrangement (Permegear® 1KM01-10, Riegelsville, Pennsylvania) was used to monitor the drug release from loaded NP. The apparatus used is shown schematically in Fig. 2. Cuprophane membrane® was used to separate donor and receiver phases in all the release studies due to its low equilibration time (McCarron et al., 2000). The sample cells were equilibrated over a period of 30 min at 37 °C and with a 1.0 ml h^{-1} flow rate

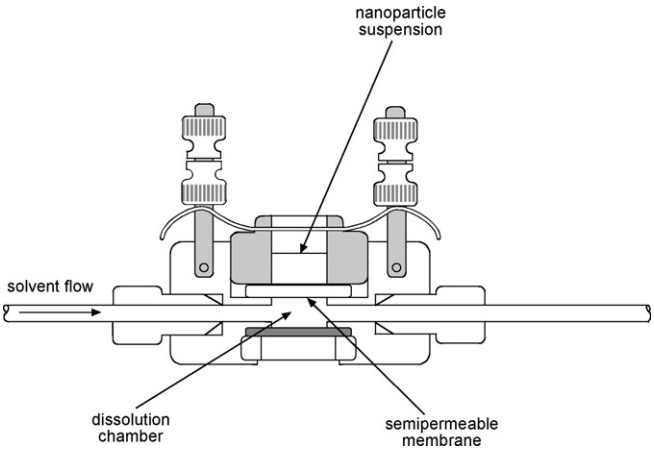

Fig. 2. Flow-through dissolution apparatus used to measure free drug flux arising from a nanoparticulate suspension held separated from a dissolution chamber by a semi-permeable membrane. Solvent flow is maintained throughout the duration of the experiment, allowing fractions of eluate to be collected in a periodic fashion.

of phosphate-buffered saline (PBS), the latter driven using a modified triple-barrelled syringe pump (Harvard Apparatus Inc., Holliston, Massachusetts).

Achieving sink conditions on the receiver side of the membrane depends on a flow rate that is sufficient to remove all permeated drug. For this work, an eluent flow rate of 1 ml h^{-1} was shown (data not shown) to achieve these conditions. A 10 mg sample of freeze-dried NP was re-suspended in 1 ml of PBS, introduced into the donor compartment of the cell and samples of eluate, again running at 1 ml h^{-1}, collected every 20 min. Sodium hydroxide (0.1 ml, 1.0 M) was added 30 min before analysis to bring about hydrolysis of prodrugs to 5FU.

The rate of change of drug concentration in the receiver phase, dC_{rec}/dt, can be calculated using Eq. (2) (Choi and Angello, 1994), which assumes instantaneous mixing in the receiver cell:

$$\frac{dC_{rec}}{dt} = \frac{AJ}{V} - \frac{F_{rec}C_{rec}}{V} \quad (2)$$

Hence, the flux, J, can be calculated by rearrangement, as shown in Eq. (3):

$$J = \frac{(V_{rec}(dC_{rec}/dt)) + (F_{rec}C_{rec})}{A} \quad (3)$$

where C_{rec} is the concentration of drug in a receiver cell of volume V, flow rate F_{rec} and cross-sectional area A. The flux for prodrug release across the semipermeable membrane was used as a measure of drug release from the nanoparticulate systems.

2.7. Statistical analysis

The Student's t-test was used for statistical analysis when two different data sets or values were compared, with a p value of less than 0.05 considered statistically significant. Where appropriate, a one-way analysis of variance (ANOVA) was used to determine differences among three or more independent groups. Post hoc comparisons were made using Tukey's HSD test. In all cases $p < 0.05$ denoted significance.

3. Results

3.1. Stabilities of prodrugs and 5FU

Base-catalysed liberation of 5FU from its 1-alkylcarbonyloxymethyl prodrug was used as the preliminary step in determining nanoparticulate loading in this study. As part of the assay validation procedure, the stability of 5FU in 1 M sodium hydroxide was evaluated over an appropriate time period relevant to that taken for the analytical procedure. As can be seen in Fig. 3(a), degradation was observed to occur, such that approximately 4% of the 5FU in a 50 μg ml^{-1} solution was lost in 2 h.

In order to determine the length of time necessary to generate 5FU fully from prodrug concentrations in both supernatant and pellet fractions, the C_7 formulation was used. As this prodrug is considered to be amongst the most hydrolytically stable in the group, the time taken for its complete conversion to 5FU was considered to be more than sufficient for that used with other homologues. The limit of quantification of 5FU (in mobile phase) was found to be approximately 50 ng ml^{-1}, which was

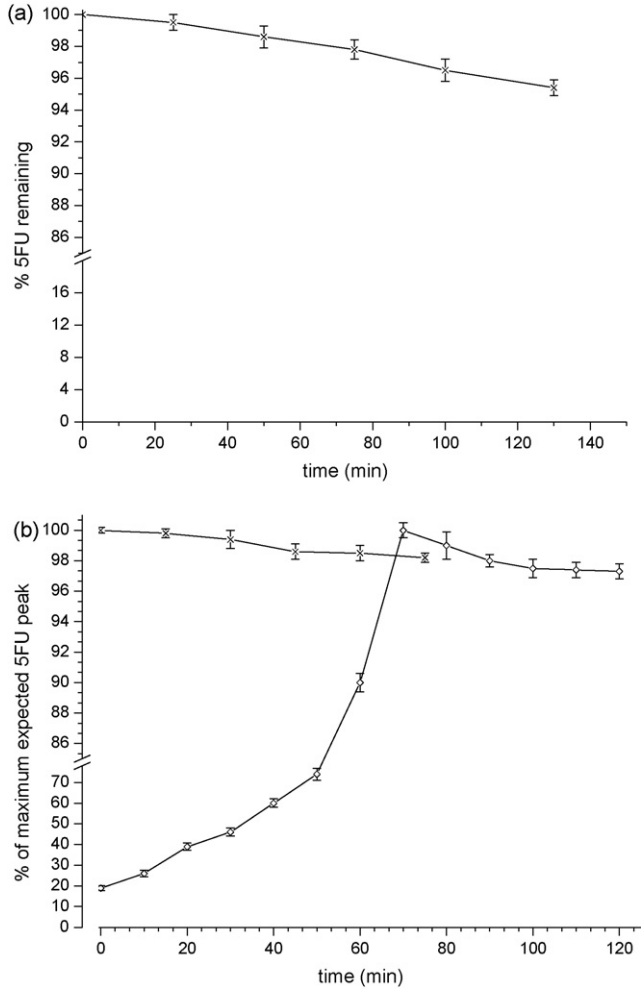

Fig. 3. (a) Degradation profile of 5FU (50 μg ml^{-1}) in 1.0 M sodium hydroxide (mean ± standard deviation; $n = 5$). (b) Base-catalysed generation of 5FU from the C_7 prodrug contained within the supernatant fraction (×) and the pellet fraction (◊) following treatment with sodium hydroxide.

Table 1
Preliminary loading study of the prodrug series

Prodrug type	Concentration of prodrug in supernatant		Concentration of prodrug in pellet	
	Observed[a] ($\mu g\,ml^{-1}$)	Mean percentage of theoretical	Observed[a] ($\mu g\,mg^{-1}$)	Mean percentage of theoretical
5FU	476.21 ± 5.35	95.24	1.84 ± 0.04	3.68
C_1	177.40 ± 4.89	82.51	2.21 ± 0.11	5.49
C_3	148.08 ± 8.11	78.77	3.39 ± 0.14	9.59
C_4	149.40 ± 3.54	83.93	4.01 ± 0.25	12.04
C_5	140.86 ± 2.36	83.84	5.79 ± 0.51	18.38
C_7	98.14 ± 1.20	64.99	13.42 ± 0.12	47.23
C_9	34.98 ± 1.25	25.35	6.53 ± 1.89	25.23

[a] Mean concentration ± S.D. ($n = 3$).

sufficiently sensitive to allow accurate determination of 5FU released following hydrolysis. Hydrolysis of the C_7 supernatant sample, as shown in Fig. 3(b), demonstrated that it was almost immediate upon NaOH addition, with the maximum possible peak area obtained for 5FU taken as the 100% value. A similar study performed on the pellet of a C_7-loaded nanoparticulate suspension is also shown in Fig. 3(b). These results confirm that 70 min is required to bring about complete liberation of 5FU. Further to this finding, it is clear from Fig. 3 that over this timeframe, 2% 5FU degradation is to be expected. Hence, these results show that a 2% level of error is introduced over the analysis period due to base-catalysed degradation.

3.2. Nanoparticulate prodrug loadings

Drug loading for all prodrugs (C_1, C_3, C_4, C_5, C_7 and C_9) are shown in Table 1, together with the amount of non-loaded prodrug still remaining in the supernatant. Loading of 5FU is poor, achieving 3.68% in the pellet, which is drug considered to be tightly associated with its polymeric matrix and resistant to conditions of moderate washing. The loading climbed steadily as the alkyl chain length increased and found to peak at C_7. Further increases did not result in additional loading, as seen with the C_9 prodrug.

The pattern of prodrug concentrations remaining in the supernatant showed a trend that was more difficult to interpret. There was no significant difference ($p > 0.5$) between the unbound concentrations found for the C_1, C_4 and C_5 derivatives and whilst significance ($p < 0.5$) was observed between mean contents for all C_1–C_5 derivatives and 5FU, the pattern follows no discernable trend. There was, however, a noticeable decrease observed upon using the C_7 prodrug, a finding that was also reflected in the changing pattern in the pellet recoveries, where higher pellet loadings generally corresponded to lower supernatant levels.

The results in Table 1 indicate that the most promising candidates for inclusion are the C_5, C_7 and C_9 prodrugs. Therefore, the stability of dry NP loaded with these payloads was evaluated further, at room and an elevated temperature, with recoveries shown during a period of 3 months (Table 2). The loadings of the C_5 and C_7 prodrugs in the NP remain within 5% of their respective initial loading, as judged using the amount of 5FU recovered after hydrolysis. The C_9 prodrugs did indicate some stability loss, especially after the longest storage interval.

Table 2
Stability of prodrug-loaded PLGA nanoparticles at 25 and 37 °C (mean ± S.D., $n = 3$)

Prodrug	Percentage of initial loading after		
	28 days	56 days	84 days
25 °C			
5FU	101.1 ± 0.9	98.5 ± 1.0	98.9 ± 1.5
C_5	100.2 ± 0.4	98.6 ± 3.0	98.1 ± 1.9
C_7	99.3 ± 1.4	96.9 ± 0.9	97.2 ± 2.0
C_9	98.7 ± 2.0	95.8 ± 1.3	94.9 ± 2.9
37 °C			
5FU	100.5 ± 1.1	99.8 ± 1.3	99.1 ± 1.4
C_5	98.2 ± 0.8	97.9 ± 0.1	96.5 ± 1.9
C_7	98.8 ± 2.4	99.0 ± 0.0	99.7 ± 2.2
C_9	95.9 ± 2.5	94.8 ± 2.6	94.0 ± 4.0

3.3. Sizing, zeta potential and polydispersity analyses

Results of sizing, zeta potential and polydispersity analyses are shown in Table 3. Little variation was seen between the various prodrug-loaded NP, with perhaps a marginally higher diameter and reduced zeta potential observed when compared to blank NP. This may be due to some surface adsorption of drug. Polydispersity was low with all batches tested, with values lower than that found in size standards (0.08) reported. No significant differences were found between the size, zeta potential and polydispersities of the NP loaded with the different prodrug types.

Table 3
Physiochemical characteristics of blank and prodrug-loaded nanoparticles (mean ± S.D., $n = 5$)

Prodrug	Size (nm ± S.D.)	Zeta potential (mV ± S.D.)	Polydispersity (±S.D.)
Blank	179.6 ± 4.1	−38.4 ± 2.8	0.045 ± 0.024
C_1	181.4 ± 3.2	−30.1 ± 2.0	0.054 ± 0.019
C_3	186.1 ± 1.2	−32.1 ± 3.4	0.043 ± 0.037
C_4	183.1 ± 5.0	−35.2 ± 1.8	0.050 ± 0.048
C_5	189.4 ± 4.2	−32.4 ± 3.4	0.054 ± 0.018
C_7	185.6 ± 3.7	−31.6 ± 3.3	0.048 ± 0.022
C_9	183.4 ± 5.6	−33.0 ± 4.1	0.062 ± 0.074

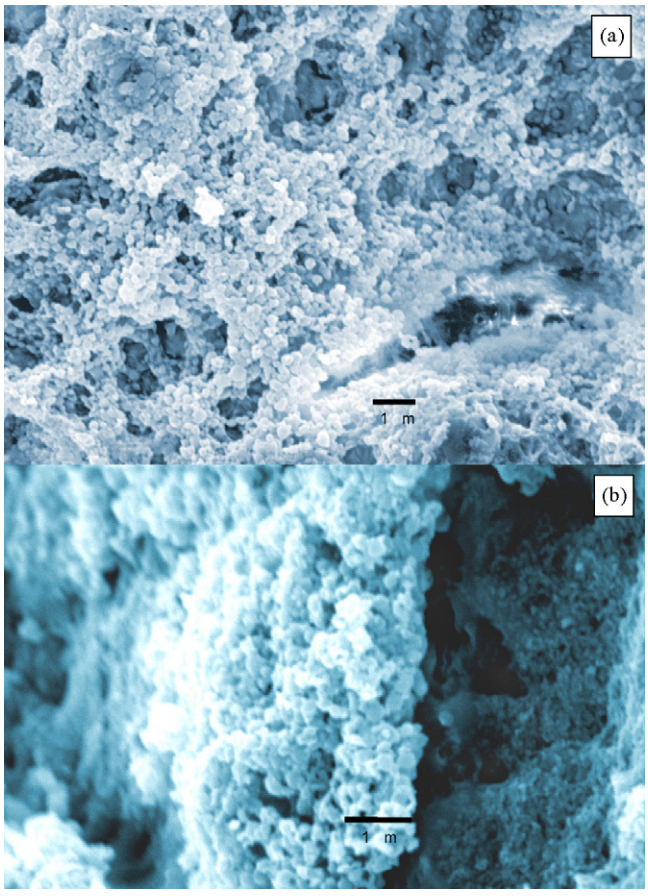

Fig. 4. SEM image of freeze-dried nanoparticles loaded with the C_7 prodrug viewed at (a) 4500× and (b) 7500× magnifications.

3.4. Scanning electron microscopy

SEM images of lyophilised NP loaded with the C_7 prodrug are shown in Fig. 4. The process of freeze-drying brought about extensive aggregation, although discrete NP are discernible. NP had a smooth surface, with no obvious signs of adsorbed drug present and are mostly of regular spherical shape. Their size correlates well with that found using photon correlation spectroscopy, being around 200 nm in diameter.

3.5. Drug release

The cumulative percentage drug release from NP loaded with the C_5 prodrug is shown in Fig. 6(a). The release was linear over the first 6 h, with no evidence of a burst effect. Approximately 14% of the total drug associated with the NP was released over the 6 h of the study. The flux profile of the C_5 loaded NP is shown in Fig. 7(a). After an initial peak in flux in the first sampling interval, the flux decreases rapidly and becomes almost linear for the remainder of the release.

The release from NP loaded with the C_7 prodrug is shown in Fig. 5(b). While the release profile has the same linear nature as the C_5 prodrug, the rate of release is considerably less, with only 4% of the drug released in 6 h. The flux of the C_7 prodrug from the prodrug-loaded NP is shown in Fig. 6(b). A similar pattern

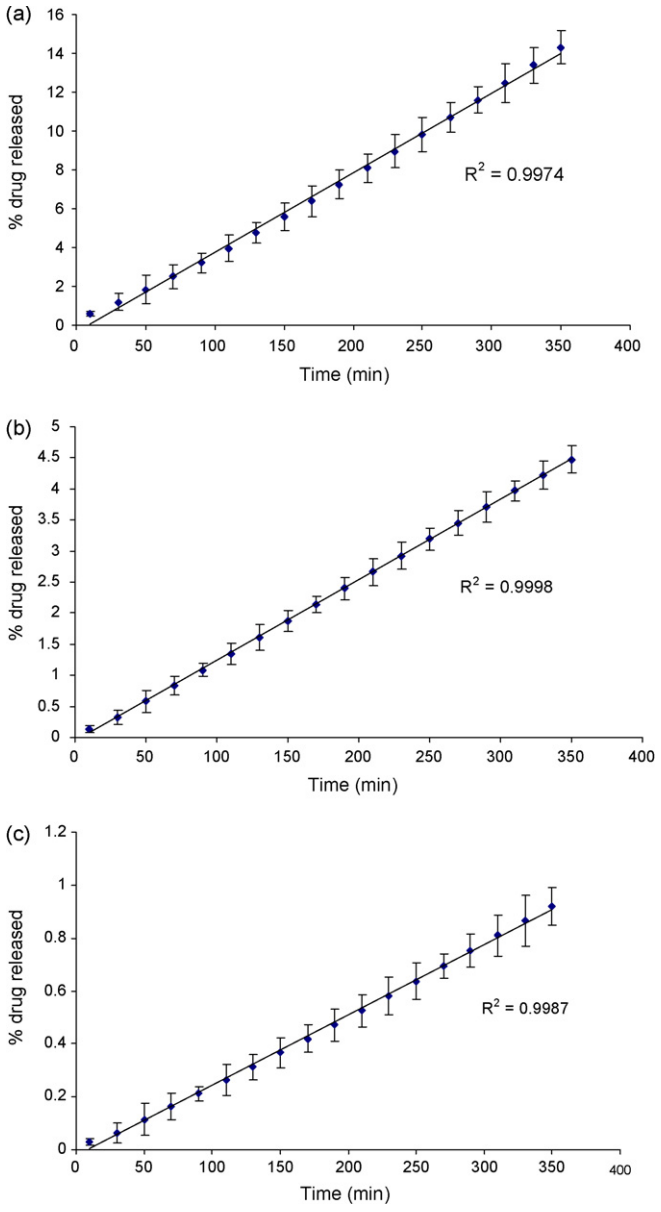

Fig. 5. The cumulative percentage drug release from NP loaded with, (a) the C_5 prodrug, (b) the C_7 prodrug and (c) the C_9 prodrug (mean ± S.D., $n = 3$).

to the C_5 prodrug release is evident, with an initial high flux value decreasing to a steady, linear profile. Finally, the cumulative percentage drug release from C_9-loaded NP in shown in Fig. 5(c). A further decrease in the total percentage released over the 6-h release period is apparent, with less than 1% of prodrug associated with the particles being released. The same linear profile as found with the other prodrugs is also observed here. The flux profile of the C_9 prodrug from loaded NP is shown in Fig. 6(c). The initial high flux found with the other prodrugs is less pronounced, although the pattern of a constant flux for the remainder of the release is shared with the other prodrug types.

4. Discussion

Loading 5FU into a nanoparticulate carrier offers benefits in terms of sustaining intravenous release, possible entrapment in

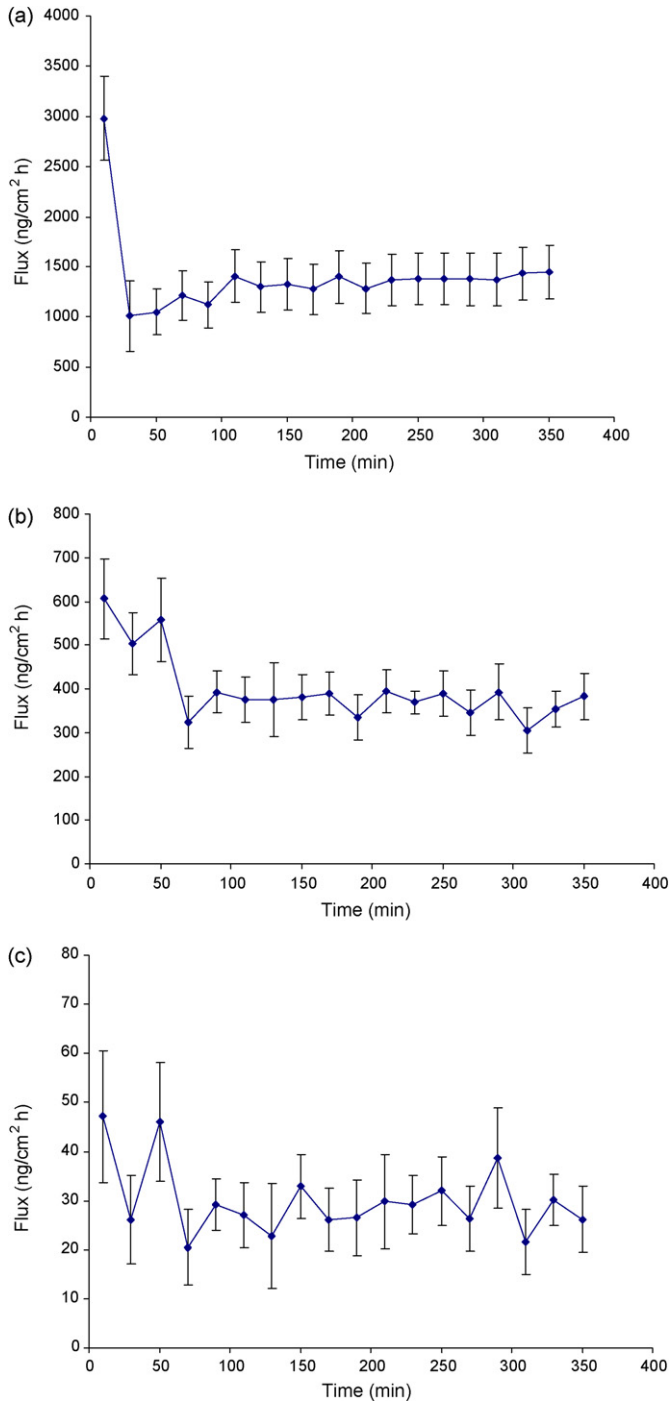

Fig. 6. Time-resolved flux profile of (a) the C_5-loaded NP, (b) the C_7-loaded NP and (c) the C_9-loaded NP (mean ± S.D., $n = 3$).

vascularised tumour tissue and alterations in pharmacokinetic profiles. It is generally accepted that lipophilic drug substances load with higher efficiencies into polymeric NP, such as those composed of PLGA. Water-soluble counterparts are more likely to remain in the aqueous continuous phase, giving high amounts of free drug in supernatant fractions. Fluorouracil is no exception and as the 5FU loading results in Table 1 confrim, its incorporation into polymeric colloidal carriers has proved arduous. The presence of heteroatoms, capable of hydrogen bonding, gives the compound its hydrophilic nature, notwithstanding a water solubility described as sparing (12.5 mg ml^{-1}). It is feasible, therefore, to propose that structural modifications of 5FU, leading to enhanced lipophilicity, may result in better nanoparticulate loading.

The prodrug strategy, as was performed in this work, is an obvious structural-based approach to facilitate enhanced loading into a particulate system, but is one that has been used infrequently. However, a small number of studies have been performed, with varied success. A greater incorporation of the anti-HIV drug 3′-azido-3′-deoxythimidine into solid lipid NP was noted when esterified with palmitic acid (Heiati et al., 1997). The parent compound gave loadings of around 1%, whereas up to a 90% loading was achieved with the prodrug (Heiati et al., 1997). Hodoshima et al. (1997) loaded the adriamycin prodrug 4′-*O*-tetrahydropyranyl-adriamycin into lipid NP, although release studies showed no benefit compared with prodrug alone. A polymeric prodrug was prepared by coupling 5-iodo-2′-deoxyuridine to poly(lactic acid) via a succinic acid spacer (Rimoli et al., 1999). The conjugate was reported to be stable in phosphate buffer at physiological pH, but able to be degraded in the presence of esterases in biological fluids (Rimoli et al., 1999). A similar approach was used by Salomone et al. (2001), who prepared cholesterol butyrate solid lipid nanospheres for the delivery of butyric acid to melanoma cell lines. What is clear from these approaches is that pendant chemical groups able to impart lipophilicity to a parent drug substance will influence nanoparticulate entrapment.

The creation of a homologous series of 1-ACOM prodrugs, as exploited in this work, is a strategy that has been used before to optimise drug delivery. For example, topical delivery of 1-ACOM prodrugs of 5FU, mercaptopurine and theophylline, and their interaction with their vehicles, has been described (Roberts and Sloan, 1999; Sloan et al., 2003; Kerr et al., 1998). Interestingly, the majority of published work evaluates these derivatives in terms of their pharmaceutical attributes and little mention is made of their native cytotoxicity. While the physiochemical characteristics of the drug are an important determinant of nanoparticulate loading, the preparatory method used in the manufacture is also a key factor. The nanoprecipitation method used in this work has ubiquitous appeal and although this technique has been used to incorporate water-soluble drugs (Barichello et al., 1999; Govender et al., 1999), loadings have been consistently poor and lipophilic drugs are normally preferred (Paul et al., 1997; Chorny et al., 2002). The method involves dissolving the drug and polymer in a water-miscible solvent, such as acetone, and then adding this solution to an aqueous medium, which may or may not contain surfactant (Govender et al., 1999; Fonseca et al., 2002). When the polymeric solution mixes with the aqueous phase, areas of super-saturation of polymer arise, which form so-called ‘proto-nanoparticles’ as solvent diffuses outwards (Quintanar-Guerrero et al., 1997). Further evaporation of organic solvent from the preparatory medium causes the polymer to harden, with the production of solid NP, as is demonstrated in Fig. 4(a) and (b). It should be noted that these images are taken of freeze-dried samples, a process that often

enhances aggregation and reductions in image quality. However, the electron micrographs demonstrate a high fraction of NP with little evidence of microparticles and associated debris. Images produced by scanning electron microscopy correlate well with results from sizing analysis using photon correlation spectroscopy, with NP diameters around 200 nm. The effect of centrifugation and freeze-drying of the particles is evident in their aggregated appearance. Some NP appear deformed from the more usual spherical shape, which may be a result of centrifugal force acting on particles with soft polymeric matrices. There is no evidence of crystals or amorphous masses of drug material, although this would be difficult to visualise in images such as these.

The results in Table 1 support the premise that increased lipophilicity enhance loading into PLGA NP, although interestingly up to a point. The 47% loading efficiency of the C_7 prodrug in comparison to the poor loading of 5FU, which was approximately 4%, demonstrates the effect of the 1-alkylcarbonyloxymethyl residue in influencing the dynamic for the prodrug to move from the aqueous into the NP matrix. Also, when the loadings of the prodrugs were compared to published data (Taylor and Sloan, 1998) regarding the hydrophilic/lipophilic balance of the compounds, a good degree of correlation can be observed, as shown in Fig. 7. The prodrugs demonstrate progressively greater water insolubility as the chain length increases, although a corresponding rise in lipophilicity reaches its maximum with the C_4 prodrug. As the *R*-group lengthens to C_7 and then to C_9, both water solubility and lipid solubility decrease markedly. This can be attributed to the increased van der Waals forces between the lengthening alkyl chains, leading to increased crystal lattice energy (Taylor and Sloan, 1998). There is a corresponding decrease in the loading of particles, which would agree with a decreased solubility in the organic phase. Prodrugs with a high water solubility and low lipid solubility tend to give low loadings, whereas those with a low hydrophilicity and enhanced lipophilicity are best suited to give optimal prodrug incorporation.

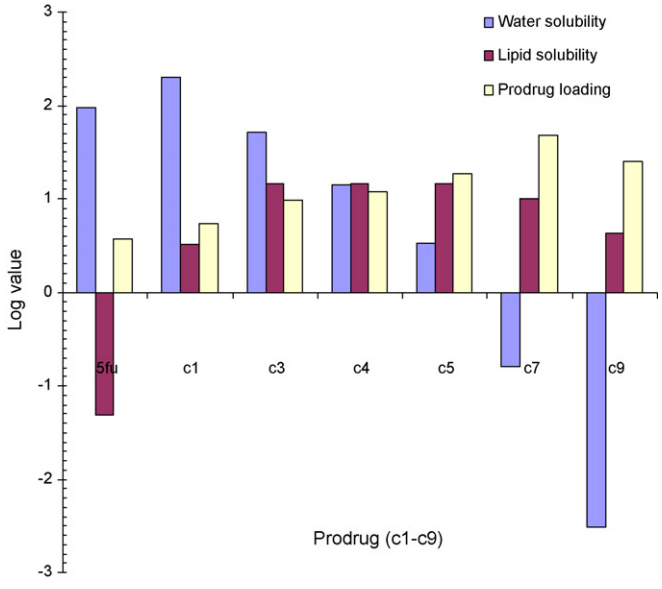

Fig. 7. Graph showing the comparison of water solubilities, lipid solubilities and drug loadings of 5FU and 1-alkylcarbonyloxymethyl prodrugs.

An important aspect to this work was the choice to hydrolyse all prodrug analogues fully to 5FU. The pH/hydrolysis profiles of the 5FU 1-ACOM prodrugs have been elucidated (Buur et al., 1985) and show a minimal rate of hydrolysis at approximately pH 5. Upon addition of strong base, hydrolysis of prodrug in the supernatant fraction occurred almost instantly, as shown in Fig. 3(b). Indeed, small quantities (approximately 1–2%) of 5FU were detected, even with the C_9 prodrug, when the supernatants were analysed prior to sodium hydroxide addition. Because of this susceptibility to hydrolysis, the evaluation of prodrug release *per se* into an aqueous receiver phase is made difficult. It was for this reason that forcing hydrolysis to completion and detection of 5FU was used. An immediate analysis of the supernatant following NaOH addition gave a 5FU concentration equivalent to 100% of the available 5FU in this phase. In effect, this is the non-incorporated prodrug, the concentration of which can be calculated from simple stoichiometry. Knowing this allows the calculation of the amount of prodrug in the nanoparticulate fraction. It is then possible to calculate the maximum prodrug release and, *ergo*, the maximum 5FU that can be generated using hydrolysis, giving the maximum 100% 5FU release from the NP.

Despite the various problems and errors associated with the use and degradation of the prodrugs, there was a definite benefit observed in all members of the homologous series in terms of drug loading. Even the C_1 prodrug, which has a greater aqueous solubility than 5FU, was more efficiently incorporated than the parent drug. The reason for this is its much greater lipid solubility, which enables the prodrug to partition into the organic phase more easily. From the results shown in Table 1 and the hydrophilic/lipophilic solubilities given in Fig. 7, it can be seen that those drugs that are loaded effectively have a reduced water solubility and a high lipid solubility. If the drug is too hydrophilic, it partitions into the aqueous phase, as is demonstrated by 5FU. If the drug has poor lipid solubility, even though it is also poorly water soluble, it still is incorporated poorly, as shown in the results of the C_9 prodrug. The best loadings are, therefore, found with the C_5 and C_7 prodrugs, which have the optimum balance between low water solubility and enhanced lipophilicity.

Results from the analysis of the various physiochemical properties (Table 3) of the NP showed little variation between different prodrug-loaded NP. Size was unrelated to prodrug loading or physiochemical characteristics, with all batches averaging around 185 nm. This low degree of variability indicates that the preparatory method for the NP is robust and reproducible. Zeta potential analysis of the prodrug NP showed a decrease from that found using blank NP. This was true for the three prodrugs examined and may be due to the masking of carbonyl groups at the NP surface by adsorbed drug. Although the zeta potential was less than −30 mV and, hence, considered a stable suspension, significant difficulty was experienced when re-suspending NP after centrifugation. It was apparent that most NP had irreversibly aggregated, which made dissolution in sodium hydroxide during the loading studies more difficult. This may be due to the incom-

plete hardening of the NP, with possible trace amounts of solvent remaining. Polydispersity results showed that the particle distribution was monomodal, with slight inter-batch variation. Most results were around 0.05, which is quoted as the polydispersity associated with standards for equipment calibration. Hence, the polydispersity results show the method of production reproducibly manufactured particles of high quality, with narrow size distributions. A stability study of the freeze-dried prodrug-loaded NP (Table 2) revealed that the dry formulations did not loose more that 5% of their initial loadings, with the possible exception of the C_9-loaded NP. Although, these results should be viewed with some caution as degradation of the respective payload will probably proceed to 5FU, which is forced upon the formulation anyway during extraction. This will inevitably mask any small amounts of underlying degradation within the NP matrix.

In this study, a novel in-line flow-through diffusion cell was used for determining drug release from the three colloidal formulations giving the highest loadings, namely the C_5, C_7 and C_9. The semi-permeable membrane, as shown in Fig. 2, allows free drug to partition into the receiver phase, which moves continuously through the cell, thus helping to maintaining sink conditions. This is seen as advantageous when compared to the more common Franz-type diffusion cells (Cordoba-Diaz et al., 2000), where a lack of renovation of receptor medium can influence the diffusion gradient in these static cell apparatus. In this study, a steady flux was achievable for 6 h (Fig. 6), but an obvious improvement to this work would be to evaluate prodrug release beyond this time. Prolonged periodic sampling is more challenging for simple flow-through cells and some form of autosampling procedure is required. Importantly, the release data in Fig. 5 do not indicate a pronounced burst effect, often typical of drug-loaded nanoparticulate systems. This would support the contention that prodrug loading seen in this study is not solely a surface binding effect, but involves molecular dispersion throughout the matrix of the NP.

In conclusion, this work has demonstrated the loading of NP with 1-ACOM prodrugs of 5FU in order to improve the level of 5FU incorporation. Compared with the parent drug, the efficiency of prodrug loading was much greater with the more lipophilic prodrugs. The greatest loadings were found with prodrugs that had the best hydrophilic–lipophilic balance, with the C_7 homologue giving loadings of over 47%. Sodium hydroxide was found to degrade the prodrugs to 5FU effectively, with a 2% loss of 5FU reported over this same period in stability studies. SEM studies revealed spherical particles of around 200 nm in diameter, corresponding well with measurements made using photon correlation spectroscopy. A narrow size distribution was produced with all the batches of particles examined, with polydispersity values under 0.08 recorded. Zeta potentials were moderately negative, with prodrug-loaded particles yielding slightly more positive results.

Acknowledgements

The authors wish to acknowledge financial support from the Research and Development Office (Northern Ireland) for providing a research scholarship for M. Hall. The authors would also like to express their gratitude to Dr. K Sloan, Dept. of Medicinal Chemistry, University of Florida, Gainsville for kindly supplying samples of the 1-ACOM prodrugs.

References

Barichello, J.M., Morishita, M., Takayama, K., Nagai, T., 1999. Encapsulation of hydrophilic and lipophilic drugs in PLGA nanoparticles by the nanoprecipitation method. Drug Dev. Ind. Pharm. 25, 471–476.

Beall, H.D., Sloan, K.B., 1996. Transdermal delivery of 5-fluorouracil (5-fu) by 1-alkylcarbonyl-5-fu prodrugs. Int. J. Pharm. 129, 203–210.

Beall, H., Prankerd, R., Sloan, K., 1994. Transdermal delivery of 5-fluorouracil (5-fu) through hairless mouse skin by 1-alkyloxycarbonyl-5-fu prodrugs: physicochemical characterization of prodrugs and correlations with transdermal delivery. Int. J. Pharm. 111, 223–233.

Bonina, F.P., Puglia, C., Barbuzzi, T., de Caprariis, P., Palagiano, F., Rimoli, M.G., Saija, A., 2001. In vitro and in vivo evaluation of polyoxyethylene esters as dermal prodrugs of ketoprofen, naproxen and diclofenac. Eur. J. Pharm. Sci. 14, 123–134.

Brigger, I., Dubernet, C., Couvreur, P., 2002. Nanoparticles in cancer therapy and diagnosis. Adv. Drug Deliv. Rev. 54, 631–651.

Bundgaard, H., Mork, N., Hoelgaard, A., 1989. Enhanced delivery of nalidixic acid through human skin via acyloxymethyl ester prodrugs. Int. J. Pharm. 55, 91–97.

Buur, A., Bundgaard, H., 1984. Prodrugs of 5-fluorouracil I. Hydrolysis kinetics and physicochemical properties of various *n*-acyl derivatives of 5-fluorouracil. Int. J. Pharm. 21, 349–364.

Buur, A., Bundgaard, H., Falch, E., 1985. Prodrugs of 5-fluorouracil. IV. Hydrolysis kinetics, bioactivation and physicochemical properties of various n-acyloxymethyl derivatives of 5-fluorouracil. Int. J. Pharm. 24, 43–60.

Buur, A., Bundgaard, H., Falch, E., 1986. Prodrugs of 5-fluorouracil VII. Hydrolysis kinetics and physicochemical properties of *n*-ethoxy- and *n*-phenoxycarbonyloxymethyl derivatives of 5-fluorouracil. Acta Pharm. Suec. 23, 205–216.

Chan, S.Y., Li Wan Po, A., 1989. Prodrugs for dermal delivery. Int. J. Pharm. 55, 1–16.

Chari, R.V.J., 1998. Targeted delivery of chemotherapeutics: tumor-activated prodrug therapy. Adv. Drug Deliv. Rev. 31, 89–104.

Choi, H.K., Angello, J.T., 1994. Mathematical analysis and optimization of a flow-through diffusion cell system. Pharm. Res. 11, 595–599.

Chorny, M., Fishbein, I., Danenberg, H.D., Golomb, G., 2002. Lipophilic drug loaded nanospheres prepared by nanoprecipitation: effect of formulation variables on size, drug recovery and release kinetics. J. Control. Release 83, 389–400.

Cordoba-Diaz, M., Nova, M., Elorza, B., Cordoba-Diaz, D., Chantres, J.R., Cordoba-Borrego, M., 2000. Validation protocol of an automated in-line flow-through diffusion equipment for in vitro permeation studies. J. Control. Release 69, 357–367.

Denny, W.A., 2001. Prodrug strategies in cancer therapy. Eur. J. Med. Chem. 36, 577–595.

Dubois, V., Dasnois, L., Lebtahi, K., Collot, F., Heylen, N., Havaux, N., Fernandez, A.-M., Lobl, T.J., Oliyai, C., Nieder, A., 2002. Cpi-0004na, a new extracellularly tumor-activated prodrug of doxorubicin: in vivo toxicity, activity, and tissue distribution confirm tumor cell selectivity. Cancer Res. 62, 2327–2331.

Fonseca, C., Simoes, S., Gaspar, R., 2002. Paclitaxel-loaded PLGA nanoparticles: preparation, physicochemical characterization and in vitro anti-tumoral activity. J. Control. Release 83, 273–286.

Govender, T., Stolnik, S., Garnett, M.C., Illum, L., Davis, S.S., 1999. PLGA nanoparticles prepared by nanoprecipitation: drug loading and release studies of a water soluble drug. J. Control. Release 57, 171–185.

Grem, J.L., 2000. 5-Fluorouracil: forty-plus and still ticking. A review of its preclinical and clinical development. Invest. New Drugs 18, 299–313.

Heiati, H., Tawashi, R., Shivers, R.R., Phillips, N.C., 1997. Solid lipid nanoparticles as drug carriers. 1. Incorporation and retention of the lipophilic prodrug 3′-azido-3′-deoxythymidine palmitate. Int. J. Pharm. 146, 123–131.

Hodoshima, N., Udagawa, C., Ando, T., Fukuyasu, H., Watanabe, H., Nakabayashi, S., 1997. Lipid nanoparticles for delivering antitumor drugs. Int. J. Pharm. 146, 81–92.

Johansen, M., Mollgaard, B., Wotton, P.K., Larsen, C., Hoelgaard, A., 1986. In vitro evaluation of dermal prodrug delivery—transport and bioconversion of a series of aliphatic esters of metronidazole. Int. J. Pharm. 32, 199–206.

Kerr, D., Roberts, W., Tebbett, I., Sloan, K.B., 1998. 7-Alkylcarbonyloxymethyl prodrugs of theophylline: topical delivery of theophylline. Int. J. Pharm. 167, 37–48.

Malet-Martino, M., Jolimaitre, P., Martino, R., 2002. The prodrugs of 5-fluorouracil. Curr. Med. Chem. Anti-Cancer Agents 2, 267–310.

McCarron, P.A., Woolfson, A.D., Keating, S.M., 1999. Response surface methodology as a predictive tool for determining the effects of preparation conditions on the physicochemical properties of poly(isobutylcyanoacrylate) nanoparticles. Int. J. Pharm. 193, 37–47.

McCarron, P.A., Woolfson, A.D., Keating, S.M., 2000. Sustained release of 5-fluorouracil from polymeric nanoparticles. J. Pharm. Pharmacol. 52, 1451–1459.

Mollgaard, B., Hoelgaard, A., Bundgaard, H., 1982. Pro-drugs as drug delivery systems. xxiii. Improved dermal delivery of 5-fluorouracil through human skin via *n*-acyloxymethyl pro-drug derivatives. Int. J. Pharm. 12, 153–162.

Paul, M., Fessi, H., Laatiris, A., Boulard, Y., Durand, R., Deniau, M., Astier, A., 1997. Pentamidine-loaded poly(D,L-lactide) nanoparticles: physicochemical properties and stability work. Int. J. Pharm. 159, 223–232.

Quintanar-Guerrero, D., Allemann, E., Doelker, E., Fessi, H., 1997. A mechanistic study of the formation of polymer nanoparticles by the emulsification-diffusion technique. Colloid Polym. Sci. 275, 640–647.

Rang, H.P., Dale, M.M., Ritter, J.M., 1995. Pharmacology. Churchill-Livingstone, New York.

Rautio, J., Nevalainen, T., Taipale, H., Vepsalainen, J., Gynther, J., Laine, K., Jarvinen, T., 2000. Piperazinylalkyl prodrugs of naproxen improve in vitro skin permeation. Eur. J. Pharm. Sci. 11, 157–163.

Rimoli, M.G., Avallone, L., de Caprariis, P., Galeone, A., Forni, F., Vandelli, M.A., 1999. Synthesis and characterisation of poly(-lactic acid)-idoxuridine conjugate. J. Control. Release 58, 61–68.

Roberts, W.J., Sloan, K.B., 1999. Correlation of aqueous and lipid solubilities with flux for prodrugs of 5-fluorouracil, theophylline, and 6-mercaptopurine: a Potts-Guy approach. J. Pharm Sci. 88, 515–522.

Salomone, B., Ponti, R., Gasco, M.R., Ugazio, E., Quaglino, P., Osella-Abate, S., Bernengo, M.G., 2001. In vitro effects of cholesteryl butyrate solid lipid nanospheres as a butyric acid pro-drug on melanoma cells: evaluation of antiproliferative activity and apoptosis induction. Clin. Exp. Metastasis 18, 663–673.

Schmoll, H.J., Buchele, T., Grothey, A., Dempke, W., 1999. Where do we stand with 5-fluorouracil? Semin. Oncol. 26, 589–605.

Sloan, K.B., Wasdo, S., Ezike-Mkparu, U., Murray, T., Nickels, D., Singh, S., Shanks, T., Tovar, J., Ulmer, K., Waranis, R., 2003. Topical delivery of 5-fluorouracil and 6-mercaptopurine by their alkylcarbonyloxymethyl prodrugs from water: vehicle effects on design of prodrugs. Pharm. Res. 20, 639–645.

Taylor, H.E., Sloan, K.B., 1998. 1-Alkylcarbonyloxymethyl prodrugs of 5-fluorouracil (5-fu): synthesis, physicochemical properties, and topical delivery of 5-fu. J. Pharm. Sci. 87, 15–20.

Yuasa, H., Matsuda, K., Gu, J., Suzuki, E., Yokouchi, I., Watanabe, J., 1996. Dose-dependent gastrointestinal absorption of 5-fluorouracil in rats in vivo. Biol. Pharm. Bull. 19, 1494–1498.